

Development of a 100 J, 10 Hz laser for compression experiments at the High Energy Density instrument at the European XFEL

Paul Mason¹, Saumyabrata Banerjee¹, Jodie Smith¹, Thomas Butcher¹, Jonathan Phillips¹, Hauke Höppner², Dominik Möller², Klaus Ertel¹, Mariastefania De Vido¹, Ian Hollingham¹, Andrew Norton¹, Stephanie Tomlinson¹, Tinesimba Zata¹, Jorge Suarez Merchan¹, Chris Hooker¹, Mike Tyldesley¹, Toma Toncian², Cristina Hernandez-Gomez¹, Chris Edwards¹, and John Collier¹

¹Central Laser Facility, STFC Rutherford Appleton Laboratory, Didcot, OX11 0QX, UK

²Institute for Radiation Physics, Helmholtz-Zentrum Dresden-Rossendorf e.V., D-01328 Dresden, Germany

(Received 27 July 2018; revised 2 October 2018; accepted 17 October 2018)

Abstract

In this paper we review the design and development of a 100 J, 10 Hz nanosecond pulsed laser, codenamed DiPOLE100X, being built at the Central Laser Facility (CLF). This 1 kW average power diode-pumped solid-state laser (DPSSL) is based on a master oscillator power amplifier (MOPA) design, which includes two cryogenic gas cooled amplifier stages based on DiPOLE multi-slab ceramic Yb:YAG amplifier technology developed at the CLF. The laser will produce pulses between 2 and 15 ns in duration with precise, arbitrarily selectable shapes, at pulse repetition rates up to 10 Hz, allowing real-time shape optimization for compression experiments. Once completed, the laser will be delivered to the European X-ray Free Electron Laser (XFEL) facility in Germany as a UK-funded contribution in kind, where it will be used to study extreme states of matter at the High Energy Density (HED) instrument.

Keywords: cryogenic lasers; diode-pumped solid-state laser; high energy lasers; laser amplifiers; Yb:YAG

1. Introduction

One of the main research goals of the High Energy Density (HED) instrument at the European X-ray Free Electron Laser (XFEL) is to study the structural and melting behaviour of materials present at the interior of extrasolar planets^[1]. To support this, a 1 kW (100 J, 10 Hz, 1030 nm) nanosecond pulsed diode-pumped solid-state laser (DPSSL) developed at the Central Laser Facility (CLF) will be delivered to the European XFEL in Hamburg, Germany as a UK-funded contribution in kind to the facility. The laser, named DiPOLE100X, will provide temporally shaped pulses, which, once frequency doubled to 515 nm and focused, will be used to undertake dynamic shock and ramp compression experiments to produce extreme states of matter, replicating the high pressure (1 TPa) and temperature (up to 10,000 K) conditions found at planetary centres. Properties of key planetary materials (phase stabilities and equations of state) will then be determined by probing using high-brightness X-ray pulses from the FEL.

DiPOLE100X is the second 100 J, 10 Hz DPSSL system designed and built by the CLF and is based on a master oscillator power amplifier (MOPA) design with multiple amplification stages. It consists of a front end, operating at 1029.5 nm with gain media at room temperature, followed by two DiPOLE multi-slab ceramic Yb:YAG cryogenic gas cooled amplifiers, a 10 J cryo-preamplifier (MA1) and a final 100 J cryo-power amplifier (MA2). Figure 1 shows a schematic of the DiPOLE100X amplifier chain.

The DiPOLE cryogenic multi-slab amplifier concept has been developed at the CLF over the past eight years. The ceramic Yb:YAG slabs are held in aerodynamically shaped vanes and heat is removed by flowing pressurized helium gas, cooled to near cryogenic temperatures (typically around 150 K), over the slab surfaces at high velocity, a technique first demonstrated on the Mercury laser at room temperature^[2]. Cryogenic cooling minimizes reabsorption loss in the Yb-system, enabling high gain and efficient energy extraction, and further improves the thermo-mechanical and thermo-optical properties of YAG, important for high-average power operation^[3]. The amplifier is pumped from both sides by 940 nm diode sources with square flat-top

Correspondence to: P. Mason, STFC, Rutherford Appleton Laboratory, Harwell Campus, Didcot, OX11 0QX, UK. Email: paul.mason@stfc.ac.uk

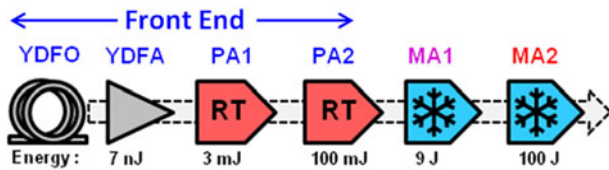


Figure 1. Schematic of DiPOLE100X amplifier chain, showing typical output energy at each amplifier stage: YDFO = Yb-silica fibre oscillator; YDFA = Yb-silica fibre amplifier (inc. temporal pulse shaping); PA = room-temperature preamplifier (1 = Yb:CaF₂ regenerative, 2 = Yb:YAG multi-pass); MA = main cryogenic amplifier (ceramic Yb:YAG multi-slab).

Table 1. Target parameters for DiPOLE100X and demonstrated performance

Parameter	Target	Demonstrated
Wavelength	1030 ± 1 nm	1029.5 nm
Pulse energy	100 J	107 J
Energy stability	<2.5% RMS	<1% RMS
Pulse rate	Single shot, 1, 2, 5 or 10 Hz	1 & 10 Hz
Jitter	<25 ps RMS	
Pulse duration	2 to 15 ns	10 ns
Pulse shape	User selectable	Flat top
Beam size & shape	75 mm square, super-Gaussian	75 mm × 77 mm, super-Gaussian ($n = 10$)
Beam quality	2 × DL	1.7 × DL (X) 2.3 × DL (Y)
Pointing stability (shot to shot)	Within ±25 μrad <4% RMS	Within ±20 μrad 1% RMS

intensity profiles to ensure a uniform gain profile. Slabs closer to the centre of the amplifier have a higher Yb-doping level to ensure a uniform thermal load in each slab, and an absorptive chromium-doped YAG cladding is added to the edge of each slab to suppress amplified spontaneous emission (ASE). Amplifier designs have been developed that produce 10 J^[4] and 100 J^[5] output at 10 Hz demonstrating the scalability of the concept.

The design of DiPOLE100X is similar to the DiPOLE100 system, the world's first kW average power, high energy, nanosecond pulsed DPSSL^[6], which is now operational at the HiLASE facility in the Czech Republic^[7], where it is being used by a growing community of scientific and industrial users for advanced materials processing and testing applications.

The main target parameters of DiPOLE100X are summarized in Table 1, along with performance values already demonstrated on DiPOLE100.

In this paper we present a progress update on the build of DiPOLE100X, highlighting design features introduced to meet the specific demands of conducting compression experiments on the HED instrument, integration of DiPOLE100X with HED infrastructure, and plans for future development of DiPOLE amplifier technology within the Centre for Advanced Laser Technologies and Applications (CALTA) at the CLF.

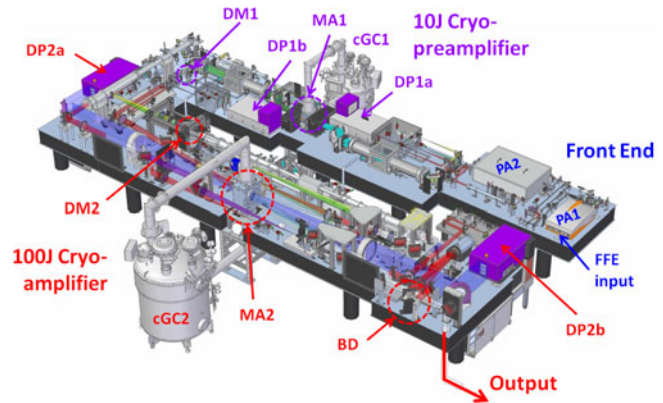


Figure 2. 3D model of DiPOLE100X: FFE = fibre front end, DP = diode pumps, cGC = cryogenic gas coolers, DM = deformable mirrors, BD = beam diverter, FFE = fibre front end (not shown).

2. Design & build

The main difference between DiPOLE100X and its predecessor is the change from a linear to U-shape folded geometry. This was necessary to reduce the footprint and fit the shape of the space available in the laser hutch at the HED instrument, and has been achieved by reorganizing and changing the direction of propagation of the beam transport (BT) section between the 10 J and 100 J cryo-amplifiers. A 3D model showing the geometry of DiPOLE100X and highlighting some of the key components of the system is given in Figure 2.

Front end

The design of the front end for DiPOLE100X is very similar to that developed for DiPOLE100^[8] and a schematic of the optical arrangement, highlighting key functional areas, is shown in Figure 3. It starts with a fibre front end (FFE) seed (IDIL Fibres Optiques, France) consisting of a (narrow linewidth) Yb-doped silica fibre oscillator (YDFO) and amplifier (YDFA) stages, followed by a fibre-coupled Mach-Zehnder lithium niobate electro-optic modulator (FEOM), which provides the temporal pulse shaping capability. To improve ASE suppression and enhance pulse contrast, particularly important for compression experiments, the FEOM in DiPOLE100X has been upgraded to a dual-stage device to provide an increased extinction ratio of >45 dB. This is then driven by a high sample rate (8 GSamples/s) arbitrary waveform generator (AWG, Kentech POPS100D) that provides 125 ps temporal resolution (200 ps rise time). All FFE components are contained in a single 6U 19-inch rack unit, which, along with the AWG, is located remotely from the front end optical table and connected via a fibre optic link.

A key component of the front end is the timing system that distributes pulses throughout the system, which need

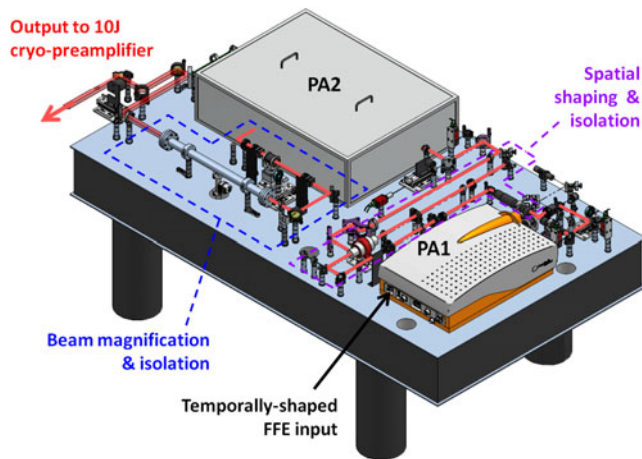


Figure 3. Schematic layout of the front end for DiPOLE100X.

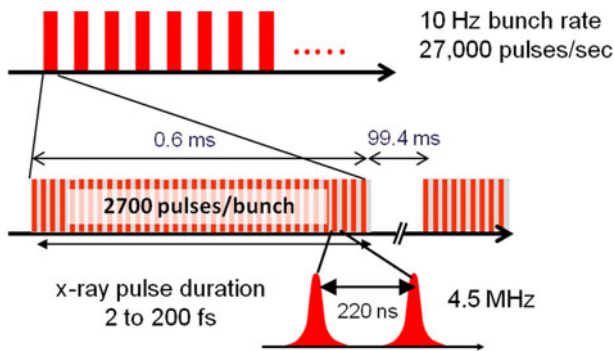


Figure 4. X-ray pulse timing diagram for SASE II beamline.

to be synchronized both internally and to the XFEL timing system. Accurate pulse timing and low jitter are particularly important to ensure reproducible synchronization with the X-ray pulse bursts. Figure 4 shows a timing diagram of the X-ray pulses produced by the SASE II beamline on the European XFEL.

To achieve accurate synchronization, DiPOLE100X has an upgraded 40-channel digital delay generator (DDG – Greenfield Technology GFT1040) that accepts two external input signals from the XFEL timing system; an 81.25 MHz signal clock derived from the XFEL master oscillator, and a 10 Hz (T_0) trigger signal synchronized with the start of each X-ray burst^[9]. Using the clock-in the DDG generates a 40.625 MHz clock signal (PA1 synchronization) and a clock-out to synchronize the delay generator of the FFE. The external 10 Hz trigger is used directly (frequency F_1) to generate a user selectable frequency at 5, 2, or 1 Hz (F_2). Every channel of the DDG produces one pulse with adjustable delay at one of these two frequencies. Finally, the XFEL timing system provides a 10 kHz trigger directly to the FFE delay generator to minimize jitter between the shaped optical pulse and X-ray pulse. The jitter between individual channels and the T_0 XFEL trigger is expected to be <20 ps

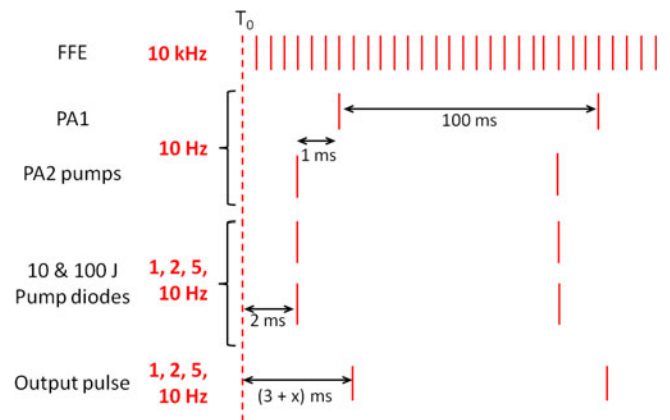


Figure 5. DiPOLE100X timing diagram.

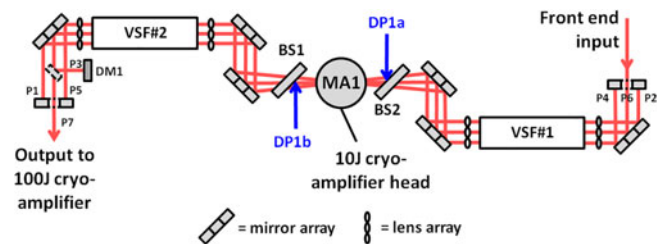


Figure 6. Schematic showing 7-pass angularly multiplexed extraction architecture of the 10 J cryo-preamplifier. DP = diode pumps, DM1 = 10 J deformable mirror, BS = beam splitters.

(RMS). A timing diagram for DiPOLE100X is shown in Figure 5.

The temporally shaped output of the FFE at 10 kHz is used to seed the Yb:CaF₂ regenerative amplifier (PA1) (custom S-PULSE supplied by Amplitude Systemes, France) producing few-mJ pulses at 10 Hz in a Gaussian spatial beam profile. The cavity length in PA1 has been increased to support the increased pulse duration range required for DiPOLE100X.

The beam is then spatially shaped into a square high-order super-Gaussian ($n > 10$) beam and relay-imaged into the Yb:YAG multi-pass amplifier (Lastronics, Germany) boosting the energy beyond 100 mJ. The output then passes through a Pockels cell to improve contrast and to pick pulses at the desired output pulse rate of the laser, if this is set to less than 10 Hz.

10 J cryo-preamplifier

The 10 J multi-pass cryo-preamplifier (MA1) design in DiPOLE100X also remains unchanged from the original. It consists of a single DiPOLE10-scale cryo-amplifier head and a seven pass angularly multiplexed extraction architecture^[5]. A schematic of the optical arrangement showing the extraction architecture is given in Figure 6. The output beam from PA2 is relay-imaged into the amplifier and on every subsequent pass by a series of vacuum spatial filters (VSFs).

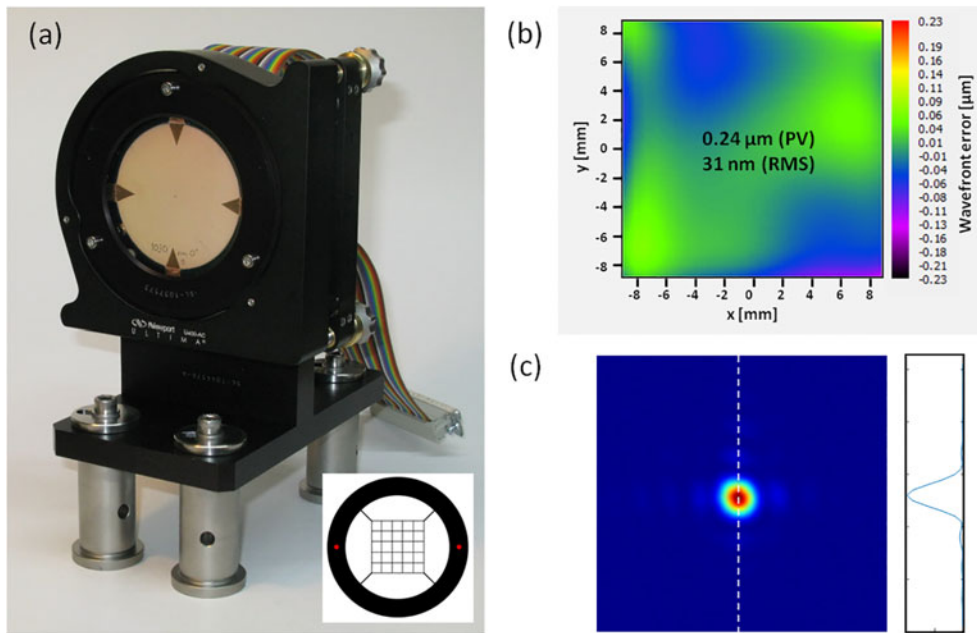


Figure 7. (a) Photograph of the DiPOLE100X 10 J bimorph deformable mirror, built at the CLF, with inset showing schematic of electrode pattern, (b) corrected output wave front and (c) far-field CCD camera image measured at 10 J, 10 Hz on the DiPOLE prototype amplifier.

Both diode-pumped lasers (Ingeneric, Germany) are coupled into the amplifier head by reflection from dielectric coated dichroic beam splitters (BSs), providing high reflection at 940 nm and high transmission at 1030 nm.

In DiPOLE100X the original deformable mirror (DM), positioned after the 3rd pass, has been replaced with a similar low-voltage bimorph-type mirror developed and built at the CLF^[10]. The DM uses a 75 mm diameter fused silica substrate, approximately 1 mm thick, bonded to a 50 mm diameter piezo-ceramic (PZT) disc, approximately 200 μm thick. Both surfaces of the fused silica substrate are coated with a high reflectivity dielectric mirror coating at 1030 nm for use at normal incidence. A photograph of the new 10 J bimorph mirror is shown in Figure 7(a). A pattern of 29 electrode actuators is applied to the rear surface of the PZT disc, consisting of a 5×5 square array similar in size to the 10 J beam (21.5 mm square), see inset of Figure 7(a), surrounded by four larger areas used primarily to control astigmatism and defocus. The design allows the mirror substrate to be removed easily, with minimal disruption, in the event that it needs to be replaced.

The mirror was tested on the DiPOLE prototype amplifier system, described elsewhere^[4], and demonstrated closed-loop correction with an output wave front error (WFE) of 0.24 μm peak to valley (PV) and 31 nm (RMS) when amplifying 10 ns duration pulses to 10 J at 10 Hz. An image of the corrected output wave front measured on the DiPOLE prototype amplifier is shown in Figure 7(b), along with the corresponding far-field image measured on a CCD camera in Figure 7(c), demonstrating near diffraction limited (DL) performance.

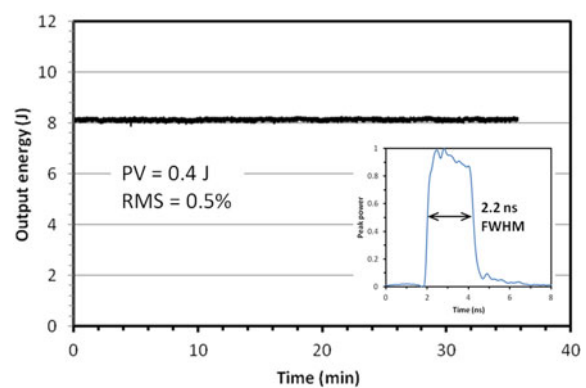


Figure 8. Energy stability over half an hour with inset showing measured temporal pulse shape for amplification of 2.2 ns pulses at 8 J, 10 Hz.

The prototype amplifier was also used to confirm reliable operation at the shorter pulse durations required for DiPOLE100X that are of interest for shock compression experiments. Output energy stability tests were undertaken for amplification of a near flat-top temporal pulse of duration 2.2 ns (FWHM) at 10 Hz, and demonstrated 8 J output with an RMS energy stability of 0.5% over half an hour operation (21,600 shots). Figure 8 shows the output energy measured over a 36 min period with the inset showing the corresponding temporal pulse profile. Although laser induced damage thresholds (LIDTs) are expected to be lower at these shorter pulse durations no evidence of optical damage was observed at the operating fluence ($\sim 2.5 \text{ J/cm}^2$) used during these tests. This gives confidence that DiPOLE100X will be able to deliver the necessary performance over the extended range of pulse durations required for HED experiments.

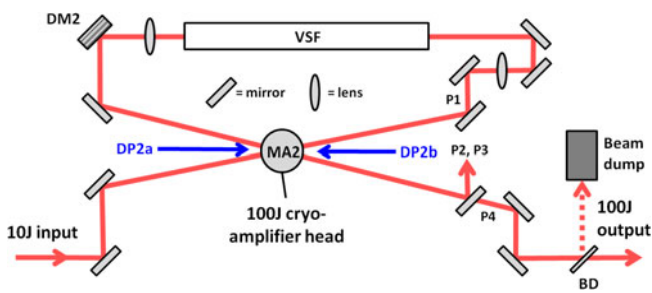


Figure 9. Schematic showing 4-pass, off-axis, angularly multiplexed extraction architecture of the 100 J cryo-amplifier. DP = diode pumps, DM2 = 100 J deformable mirror, BD = beam diverter.

The output from the 10 J cryo-preamplifier passes through a Faraday isolator before entering the beam transport section of the system. Here the polarization state and spatial orientation of the beam can be adjusted to precompensate for effects that occur in the final cryo-amplifier. The beam is then relay-imaged into a $\times 3.4$ magnification telescope to increase its size to 75 mm square ready to seed the main 100 J amplifier. The magnifying telescope is now orientated at right angles to the original design to achieve the new U-shaped layout.

100 J cryo-power amplifier

The final cryo-amplifier in DiPOLE100X also retains the same architecture used in DiPOLE100. Both diode pumps (Ingeneric, Germany) are directed into the amplifier on-axis and a 4-pass, off-axis, angularly multiplexed geometry is used to extract the stored energy^[5]. A schematic showing the extraction architecture of the 100 J cryo-amplifier is given in Figure 9.

The main change in the system is the incorporation of an upgraded DM between the first and second amplifier passes. The new DM (Imagine Optic ILAO Star 200) is based on upgraded mechanical actuator technology driven by stepper motors providing nanometric precision, now with very low hysteresis ($< 1\%$). These result in minimal backlash allowing real-time dynamic closed-loop wave front correction at up to 10 Hz. The circular mirror substrate is 200 mm in diameter and its shape is controlled by an array of 52 actuators. The mirror is mounted in a new low-profile, low distortion optical mount, a photograph of which is shown in Figure 10(a).

Prior to installation on DiPOLE100X the mirror was tested off-line as part of a closed-loop adaptive optic (AO) system, including a HASO4 Broadband-GE Shack–Hartmann wave front sensor (WFS). To confirm the mirror is able to provide smooth dynamic correction to the level required a beam of similar size and shape to the 100 J beam with an initially flat wave front was incident on the mirror. The DM was then programmed to create a wave front consistent with the level of aberration expected in the 100 J amplifier. The target wave front is shown in Figure 10(b).

After closed-loop operation the target wave front was successfully recreated with a residual error of $0.3 \mu\text{m}$ (PV) and approximately 40 nm (RMS). A map of the residual error measured is shown in Figure 7(c). This was achieved using less than 40% of the dynamic range available to the mirror actuators and gives confidence that the DM should be able to dynamically correct for the level of aberrations expected during normal operating conditions, minimizing wave front error in the 100 J output beam.

Whenever the output beam is not sent to the HED interaction area, during warm-up and testing, it is reflected off a beam diverter (BD) and absorbed in a water filled beam dump. The diverter consists of a low mass high reflectivity dielectric coated mirror mounted and attached to a linear guide providing up to 160 mm of travel. A low friction, position-encoded linear motor (Linmot, Switzerland) provides precise movement (speed and acceleration) of the mirror assembly. The diverter allows the mirror to be lowered out of, or raised into, the beam, in less than 100 ms. Movement of the diverter is synchronized to the triggering of the laser to ensure a laser pulse is not present when the mirror is travelling between positions. When the diverter mirror is in the lower position, the beam propagates through to a periscope, which in turn directs the beam downwards through the optical table into the high energy beam transport system; see Section 3.

The diverter is also used to provide the user with a single shot on demand pulse picking capability. In this mode, the front end output Pockels cell and both 10 J and 100 J cryo-amplifiers are operated at 1 Hz to maintain stable thermal conditions. When the user requests a pulse the mirror is moved out of the beam before the next available pulse arrives, and is then returned to its original position after the pulse has passed.

Control system

Control of the many components and sub-systems that make up the DiPOLE100X laser is provided by a distributed control system developed at the CLF using EPICS (Experimental Physics and Industrial Control System)^[11]. EPICS is an open source software framework, providing a collection of tools and applications for use in creating distributed control systems, which is used in many large-scale science facilities, such as particle accelerators and synchrotron light sources.

The control system is run from central Linux-based servers. Distributed access and control are provided by a graphical user interface (GUI), developed using Control System Studio (CSS) software^[12], which may be installed on any Windows-based PC connected to the system network. The user interface of the control system is broken down into a set of control screens whose functions are described in Table 2.

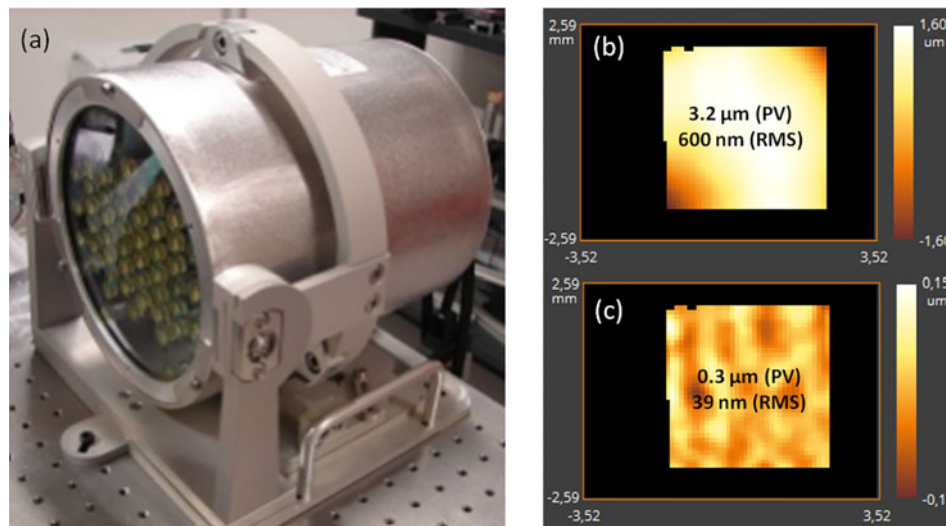


Figure 10. (a) Photograph of new 100 J deformable mirror, (b) target aberrated wave front and (c) residual error in generated wave front.

Table 2. Functionality of user control screens in DiPOLE100X control system

Control screen	Functions
Overviews	Access to summary/overview screens for each of the main sub-systems (FE, 10 J, 100 J) and the beam transport section.
Synoptics	Real-time, interactive visual displays of the status of the main sub-systems (FE, 10 J, 100 J) and their individual components. Synoptic screens use a traffic light system to indicate the status of each individual component, with green indicating that all is okay, amber indicating a component requires attention, and red indicating that either the component is off or that there is an error that requires action. Control screens can be accessed directly by touching the component symbol on-screen, minimizing the number of actions needed to view and adjust settings. An example synoptic display for the 10 J cryo-pre-amplifier is shown in Figure 11.
Automation	Useful information related to beam steering and machine safety.
Alignment	Overview of the current status of the automatic beam alignment system at various points within the system based on data from relevant near- and far-field diagnostic cameras. Again a traffic light system is used to indicate alignment status.
Interlock	Status of system interlocks.
Hazards	Important information on the status of all laser hazards. This screen can also be displayed on a remote monitor, sited outside the laser laboratory, to show whether it is safe to enter the area.

A separate programmable logic controller (PLC) provides local system monitoring and control, simultaneously providing local machine safety, sequencing components, and periodically publishing process variables (PVs) to EPICS, such that the master system is aware of each sub-systems status. A separate archiving toolset is included in EPICS that automatically records requested PVs as a function of time and stores them to disk for later retrieval.

Personnel safety is paramount, and a separate personnel safety system monitors the condition and operation of a number of interlocks. These provide a means of shutting the system down in an emergency situation through connection to the laboratory safety system. The control and safety systems continuously perform checks to prevent operation unless all safety criteria are met.

Temporal pulse shaping

Shock and ramp compression experiments require precise control of laser pulse shape. To achieve this DiPOLE100X

will incorporate a dynamic closed-loop temporal pulse shaping capability to account for the various nonlinear factors (saturation characteristics) that affect the pulse as it passes through the amplifier chain. The approach adopted uses an initial empirical estimate of the seed pulse shape, which is applied to the FEOM in the FFE via the AWG. The generated optical pulse is then amplified by the laser chain and its shape detected at the output by the combination of a high bandwidth fibre-coupled InGaAs PIN photo detector (CIM Model ISIS PHB-AJ-24E, rise & fall time <70 ps, cut-off frequency >5 GHz) and digital storage oscilloscope (Rhode & Schwarz RTO2044, 4 GHz, 4-channel, 20 GSa/s per channel). The output pulse shape is then compared to the target shape in software and a correction calculated by a custom pulse shaping algorithm developed in-house. The corrected pulse shape is then reapplied to the FEOM by the AWG. The process is then repeated over a series of iterations until the target pulse shape is reached within defined acceptance criteria.

The accuracy of shape reproduction is dependent on several factors, including the stability, resolution, and

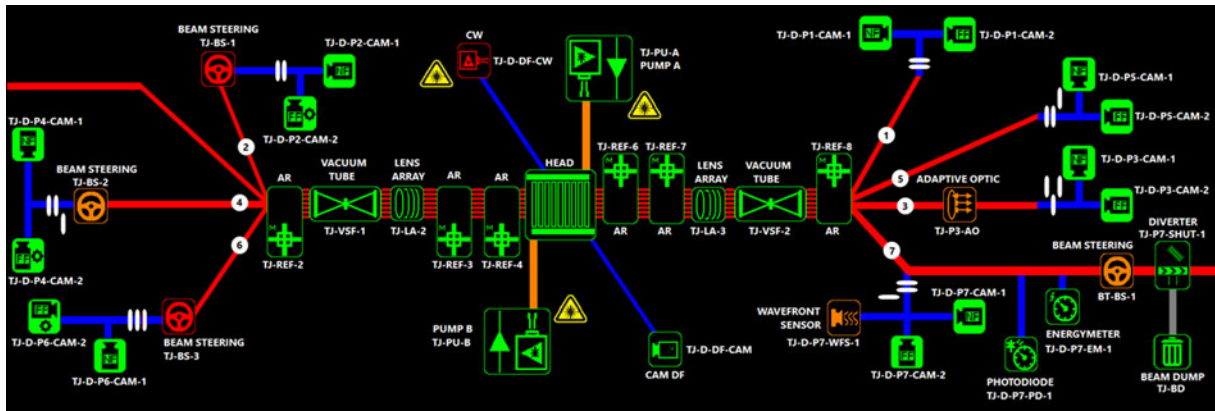


Figure 11. Synoptic screen for control and monitoring of 10 J cryo-preamplifier. Red lines correspond to the main 1030 nm laser beam path, input from the FE (left) and output to the beam transport section (right); blue lines represent diagnostic beam paths; and orange lines correspond to 940 nm pump diode beam paths.

bandwidth of the AWG and FEOM, the energy stability of the laser chain, and the noise and jitter of the detection and signal acquisition system. The pulse contrast achievable is limited by the dynamic range of the FEOM and residual ASE. To control the speed at which the pulse shape converges to the target solution, and minimize the risk of optical damage due to rapid pulse shape changes, a damping factor is included in the calculation with the aim of reaching the target shape within five to ten iterations when operated at maximum pulse rate (10 Hz).

Prior to commissioning on DiPOLE100X, the DiPOLE prototype amplifier has been used to test the pulse shaping software and optimize the algorithm in a representative amplifier chain. Results of two tests undertaken at an output energy of 6.5 J at 10 Hz are shown in Figure 12. In the first, Figure 12(a), a 10 ns duration flat-top profile with gently sloping leading and trailing edges is generated after five closed-cycle iterations, the correction on each iteration shown by the different coloured curves. The second test, Figure 12(b), demonstrates a more complex multi-step pyramid pulse shape of duration 4.5 ns FWHM obtained after ten iterations.

These results demonstrate the temporal pulse shaping capability expected from DiPOLE100X and confirm the potential to undertake dynamic single shock (flat top, high temperature, ramp low temperature) and multiple-shock (step pulse) compression experiments on the HED instrument.

Build status

Build of DiPOLE100X at the CLF commenced in March 2017 with installation of the optical tables in the laboratory. Installation of front end components was completed in May 2017 with first pulsed operation demonstrated in June 2017. The main 10 J sub-systems (pump diodes, amplifier head and cryo-cooling system) were installed at the end of September

2017 followed by all opto-mechanical components by March 2018. Full alignment of the 10 J was completed in May 2018 and pulsed commissioning is now underway. All the main 100 J sub-systems were installed by January 2018 and the majority of opto-mechanical components by June 2018. Alignment of the 100 J is scheduled to commence in July 2018 with pulsed commissioning of the full system beginning in August 2018. Control system integration and machine safety testing have occurred throughout the build with final commissioning occurring in parallel with final pulsed operation tests. At the time of writing, the build is expected to be completed by the end of September 2018.

A collection of time lapse photographs showing build progression over the past 15 months is shown in Figure 13, along with a 3D CAD view of the completed system.

3. Integration at HED instrument

The HED instrument at the European XFEL is arranged with the laser bay, or hutch, on a raised floor above the interaction area where the X-ray probe beam from the SASE II beamline enters. A schematic of the main components of the HED instrument is shown in Figure 14.

The laser hutch contains the two main lasers; the high energy (HE) nanosecond pulsed laser, DiPOLE100X that will be used for dynamic compression experiments, and a commercial high intensity (HI) laser from Amplitude Technologies (>300 TW, 25 fs, Ti:S), which will be used to study relativistic plasmas. DiPOLE100X occupies approximately half the floor area of the laser hutch with ancillary control racks, chillers and the 100 J cryostat located in a separate plant room. An HE beam transport system relay-images the output beam from DiPOLE100X beneath the floor of the laser hutch and down to an optical table alongside the interaction chamber. There it will be frequency doubled to 515 nm before being focused using phase plates into the

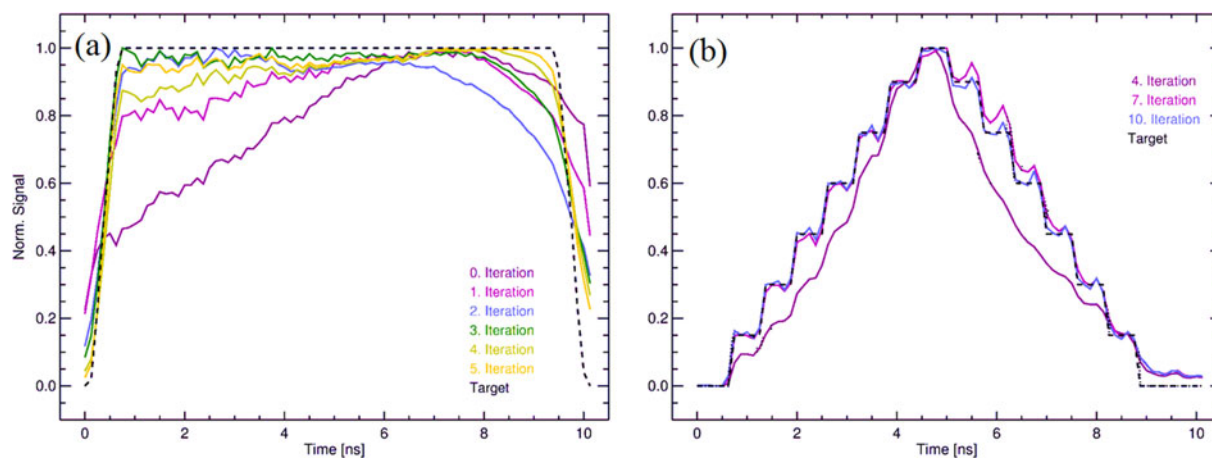


Figure 12. Temporal pulse shaping results at 6.5 J, 10 Hz obtained using the DiPOLE prototype amplifier (a) flat-top and (b) multi-step pyramid pulse profiles.

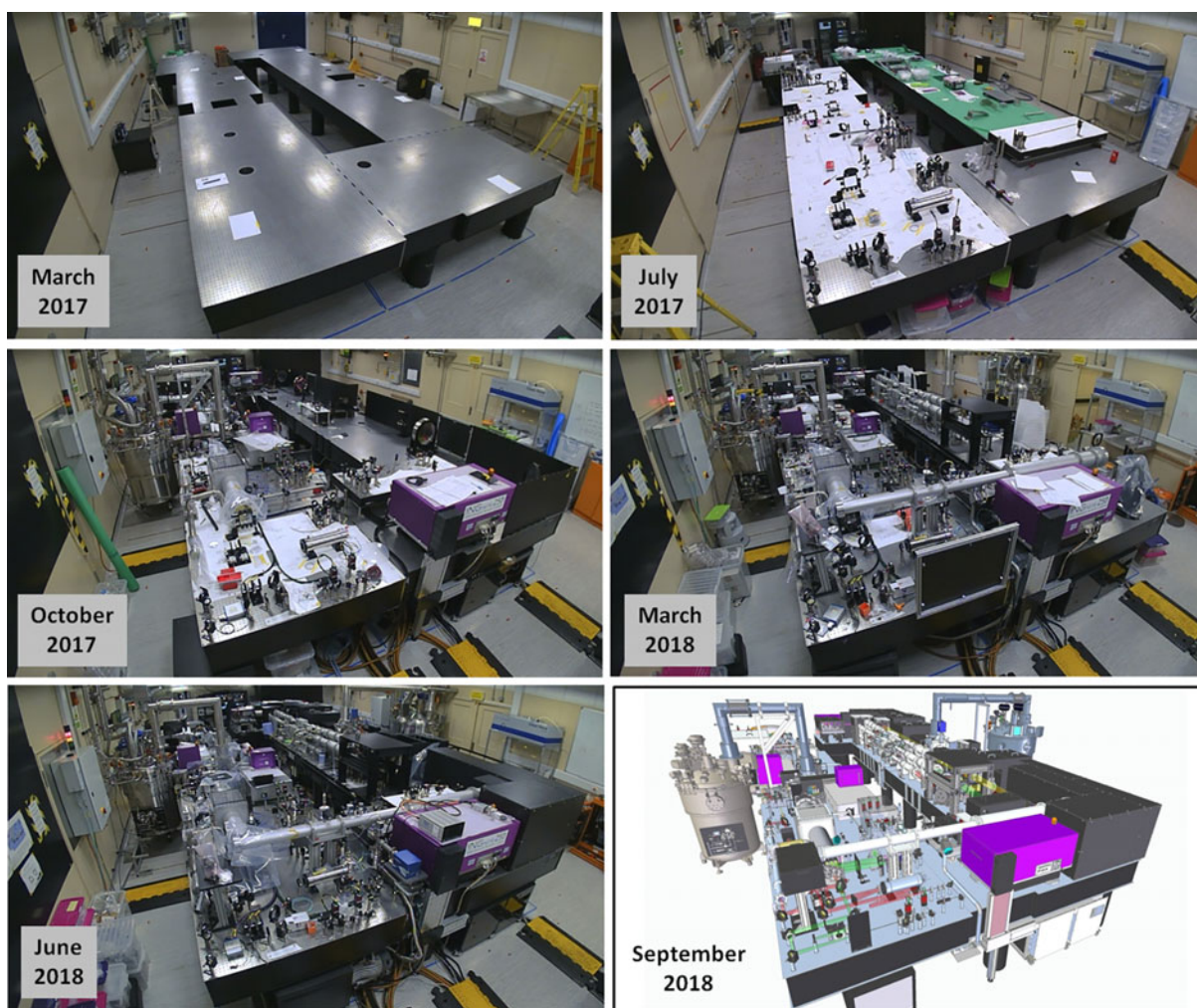


Figure 13. Time lapse photographs of DiPOLE100X build with 3D CAD view of completed system.

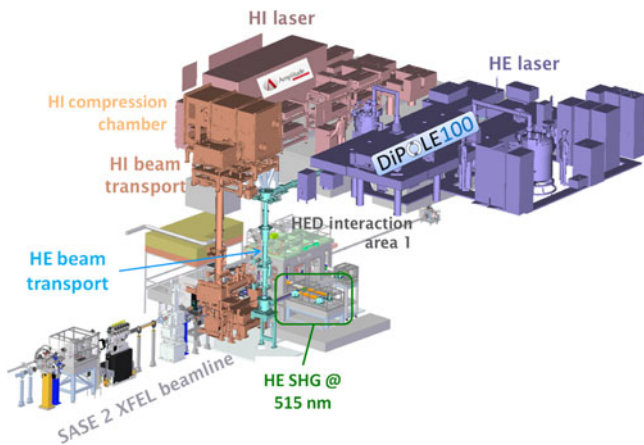


Figure 14. Schematic showing the main components of the HED instrument.

interaction chamber to achieve the desired flat-top focal intensity profile to conduct experiments. Figure 15 shows the layout of DiPOLE100X within the laser hutch and the route of the HE beam transport system.

4. Technology development

In parallel with DiPOLE100X development, separate projects within CALTA are looking at extending the performance of DiPOLE technology, demonstrating its potential for advanced materials processing applications^[13], and developing a compact pump source technology for ultra-high intensity petawatt-class lasers. These offer the potential to generate compact radiation (X-ray, γ -ray) and particle (electron, proton etc.) sources with applications in nondestructive testing, high resolution radiography^[14], and the next generation of laser plasma-based accelerators^[15].

DiPOLE technology development falls into four main research activities. The first extends the pulse repetition rate of DiPOLE from 10 Hz up to 100 Hz; the second scales the energy of the existing DiPOLE100 design towards 150 J; the third is targeted at demonstrating efficient and stable frequency conversion of DiPOLE systems into the visible (SHG at 515 nm) and UV (third harmonic generation at 343 nm), under high pulse energy and high-average power conditions; and the final activity is looking at reducing the size of DiPOLE systems.

To achieve these aims a prototype 10 J, 100 Hz DiPOLE laser is currently under development at the CLF, initially focused on industrial materials processing applications. To enable energy scaling of DiPOLE100 technology within the same design envelope work is underway to improve the damage resilience of key optical components (gain media, mirrors etc.). Furthermore, long term stability trials of SHG and THG under high-average power conditions are underway to provide extended capability for materials processing

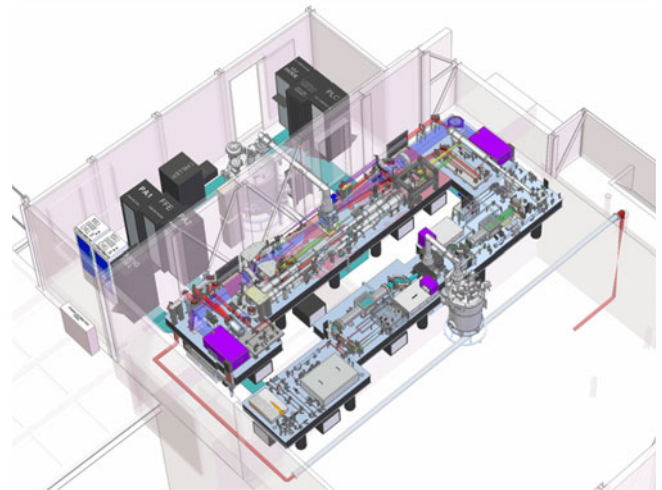


Figure 15. Layout of DiPOLE100X in laser hutch at the HED instrument.

and large beam area LIDT testing, and to demonstrate the potential of DiPOLE as a pump source technology. These activities are undertaken in collaboration with the HiLASE Facility with funding support from the Czech Republic and the European Commission^[16]. A separate internally funded project is investigating design options for size reduction of key DiPOLE component technologies (such as cryo-coolers) important for the realization of practical applications.

5. Summary

DiPOLE100X is a high energy DPSSL laser designed to produce 100 J, temporally shaped nanosecond duration pulses at up to 10 Hz in a compact geometry based on the original DiPOLE100 design. At the time of writing, all the major opto-mechanical components have been installed and commissioning of the cryo-amplifiers has begun. Testing at the CLF is scheduled for completion in autumn 2018 before shipment to the European XFEL by the end of the year.

The DiPOLE prototype amplifier has been used to confirm operation at shorter pulse durations, and the ability of DiPOLE100X to provide precisely programmed temporal pulses at up to 10 Hz repetition rate will allow determination of optimum laser pulse shapes for shock compression experiments in real time. This capability at the HED instrument, coupled with high-brightness X-ray probe pulses from the XFEL beamline, will revolutionize our understanding of the structure of materials and the processes that occur in extreme high energy density environments.

Acknowledgement

Attendance at the High Power Laser Science & Engineering (HPLSE 2018) Conference was funded by the NEWTON

China–UK Joint Research Project on Laser-driven Ion Acceleration and Novel Terahertz Radiation.

References

1. M. McMahon and U. Zastrau, *Conceptual Design Report – Dynamic Laser Compression Experiments at the HED Instrument of European XFEL*, XFEL.EU TR-2017-001, February 2017.
2. A. Bayramian, P. Armstrong, E. Ault, R. Beach, C. Bibeau, J. Caird, R. Campbell, B. Chai, J. Dawson, C. Ebbers, A. Erlandson, Y. Fei, B. Freitas, R. Kent, Z. Liao, T. Ladrán, J. Menapace, B. Molander, S. Payne, N. Peterson, M. Randles, K. Schaffers, S. Sutton, J. Tassano, S. Telford, and E. Utterback, *Fusion Sci. Technol.* **52**, 383 (2007).
3. P. D. Mason, M. Fitton, A. Lintern, S. Banerjee, K. Ertel, T. Davenne, J. Hill, S. P. Blake, P. J. Phillips, T. J. Butcher, J. M. Smith, M. De Vido, R. J. S. Greenhalgh, C. Hernandez-Gomez, and J. L. Collier, *Appl. Opt.* **54**, 4227 (2015).
4. S. Banerjee, K. Ertel, P. D. Mason, P. J. Phillips, M. De Vido, J. M. Smith, T. J. Butcher, C. Hernandez-Gomez, R. J. S. Greenhalgh, and J. L. Collier, *Opt. Express* **23**, 19542 (2015).
5. P. D. Mason, S. Banerjee, K. Ertel, P. J. Phillips, T. J. Butcher, J. M. Smith, M. De Vido, S. Tomlinson, O. Chekhlov, W. Shaikh, S. Blake, P. Holligan, M. Divoky, J. Pilar, C. Hernandez-Gomez, R. J. S. Greenhalgh, and J. L. Collier, *Proc. SPIE* **9513**, 951302 (2015).
6. P. D. Mason, M. Divoký, K. Ertel, J. Pilař, T. Butcher, M. Hanuš, S. Banerjee, P. J. Phillips, J. Smith, M. De Vido, A. Lucianetti, C. Hernandez-Gomez, C. Edwards, T. Mocek, and J. Collier, *Optica* **4**, 438 (2017).
7. O. Novák, T. Miura, M. Smrž, M. Chyla, S. S. Nagisetty, J. Mužík, J. Linnemann, H. Turčičová, V. Jambunathan, O. Slezák, M. Sawicka-Chyla, J. Pilař, S. Bonora, M. Divoký, J. Měsíček, A. Pranovich, P. Sikocinski, J. Huynh, P. Severová, P. Navrátil, D. Vojna, L. Horáčková, K. Mann, A. Lucianetti, A. Endo, D. Rostohar, and T. Mocek, *Appl. Sci.* **5**, 637 (2015).
8. T. Butcher, P. D. Mason, S. Banerjee, J. Pilar, M. Divoky, J. Smith, M. De Vido, J. Phillips, K. Ertel, O. Chekhlov, S. Tomlinson, W. Shaikh, J. Greenhalgh, I. Musgrave, C. Hernandez-Gomez, and J. Collier, in *Advanced Solid State Lasers* (OSA Technical Digest, 2014), paper ATh2A.50.
9. G. Priebe, U. Zastrau, and M. Lederer, *Timing Interfacing between XFEL and HIBEF User Consortium*, XFEL.EU 21-04-2016-3, April 2016.
10. C. J. Hooker, J. L. Collier, S. J. Hawkes, and C. Spindloe, *Central Laser Facility Annual Report 2005/6*, (2006), p. 202.
11. M. R. Kraimer, J. B. Anderson, A. N. Johnson, W. E. Norum, J. O. Hill, R. Lange, B. Franksen, and P. Denison, *EPICS Application Developer's Guide*, EPICS Base Release 3.14.12.5, 6 October 2016. <https://epics.anl.gov/index.php>.
12. <http://controlsystemstudio.org/>.
13. J. Nygaard, *The Laser User* **86**, 22 (2017).
14. C. M. Brenner, S. R. Mirfayzi, D. R. Rusby, C. Armstrong, A. Alejo, L. A. Wilson, R. Clarke, H. Ahmed, N. M. H. Butler, D. Haddock, A. Higginson, A. McClymont, C. Murphy, M. Nottley, P. Oliver, R. Allott, C. Hernandez-Gomez, S. Kar, P. McKenna, and D. Neely, *Plasma Phys. Control. Fusion* **58**, 014039 (2016).
15. P. A. Walker, P. D. Alesini, A. S. Alexandrova, M. P. Anania, N. E. Andreev, I. Andriyash, A. Aschikhin, R. W. Assmann, T. Audet, A. Bacci, I. F. Barna, A. Beaton, A. Beck, A. Beluze, A. Bernhard, S. Bielawski, F. G. Bisesto, J. Boedewadt, F. Brandi, O. Bringer, R. Brinkmann, E. Bründermann, M. Büscher, M. Bussmann, G. C. Bussolino, A. Chance, J. C. Chanteloup, M. Chen, E. Chiodroni, A. Cianchi, J. Clarke, J. Cole, M. E. Couprie, M. Croia, B. Cros, J. Dale, G. Dattoli, N. Delerue, O. Delferriere, P. Delinikolas, J. Dias, U. Dorda, K. Ertel, A. Ferran Pousa, M. Ferrario, F. Filippi, J. Fils, R. Fiorito, R. A. Fonseca, M. Galimberti, A. Gallo, D. Garzella, P. Gastinel, D. Giove, A. Giribono, L. A. Gizzi, F. J. Grüner, A. F. Habib, L. C. Haefner, T. Heinemann, B. Hidding, B. J. Holzer, S. M. Hooker, T. Hosokai, A. Irman, D. A. Jaroszynski, S. Jaster-Merz, C. Joshi, M. C. Kaluza, M. Kando, O. S. Karger, S. Karsch, E. Khazanov, D. Khikhlikha, A. Knetsch, D. Kocon, P. Koester, O. Kononenko, G. Korn, I. Kostyukov, L. Labate, C. Lechner, W. P. Leemans, A. Lehrach, F. Y. Li, X. Li, V. Libov, A. Lifschitz, V. Litvinenko, W. Lu, A. R. Maier, V. Malka, G. G. Manahan, S. P. D. Mangles, B. Marchetti, A. Marocchino, A. Martinez de la Ossa, J. L. Martins, F. Massimo, F. Mathieu, G. Maynard, T. J. Mehrling, A. Y. Molodozhentsev, A. Mosnier, A. Mostacci, A. S. Mueller, Z. Najmudin, P. A. P. Nghiem, F. Nguyen, P. Niknejadi, J. Osterhoff, D. Papadopoulos, B. Patrizi, R. Pattathil, V. Petrillo, M. A. Pocsai, K. Poder, R. Pompili, L. Pribyl, D. Pugacheva, S. Romeo, A. R. Rossi, E. Roussel, A. A. Sahai, P. Scherkl, U. Schramm, C. B. Schroeder, J. Schwindling, J. Scifo, L. Serafini, Z. M. Sheng, L. O. Silva, T. Silva, C. Simon, U. Sinha, A. Specka, M. J. V. Streeter, E. N. Svystun, D. Symes, C. Szwaj, G. Tauscher, A. G. R. Thomas, N. Thompson, G. Toci, P. Tomassini, C. Vaccarezza, M. Vannini, J. M. Vieira, F. Villa, C.-G. Wahlström, R. Walczak, M. K. Weikum, C. P. Welsch, C. Wiemann, J. Wolfenden, G. Xia, M. Yabashi, L. Yu, J. Zhu, and A. Zigler, *J. Phys. Conf. Ser.* **874**, 012029 (2017).
16. Supported by the state budget of the Czech Republic (projects LO 1602, LM2015086).